Int. J. Electrochem. Sci., 17 **(2022)** Article Number: 220727, doi: 10.20964/2022.07.13

International Journal of
ELECTROCHEMICAL
SCIENCE
www.electrochemsci.org

Electrodeposition of Ni-W/TiO_2 Composite Coatings on Q345 Pipeline Steel and their Corrosion Resistance and Anti-fouling Performance in Simulated Oilfield Wastewater

Yahong Li[*], *Yuqin Zhu*

College of Chemistry & Chemical Engineering, Xi'an Shiyou University, Xi'an 710065, China
[*]E-mail: yhli_7100@163.com

Received: 5 March 2022 / *Accepted:* 18 April 2022 / *Published:* 6 June 2022

Ni-W/TiO_2 composite coatings were electrodeposited on the surface of Q345 pipeline steel, and the corrosion resistance and anti-fouling performance of the composite coatings in simulated oilfield wastewater were studied. The results show that the concentration of TiO_2 particles in the solution has a certain influence on the composition, surface morphology, contact angle and surface free energy of the Ni-W/TiO_2 composite coating, resulting in obvious differences in the corrosion resistance and anti-fouling performance. Within a certain range, as the concentration of TiO_2 particles increases, the amount of TiO_2 particles doped in the composite coating increases, which can effectively reduce the activation energy of crystal nucleation and promote nucleation, so that the surface of the composite coating tends to be compact. The Ni-W/TiO_2 composite coating prepared with the concentration of TiO_2 particles 4 g/L has tight bonding and compact surface with the highest TiO_2 particle content of 3.90%, the lowest surface free energy of 25.48 mN/m and the largest contact angle of 120°, which can effectively improve the corrosion resistance and anti-fouling performance of Q345 pipeline steel in simulated oilfield wastewater.

Keywords: Q345 pipeline steel; Ni-W/TiO_2 composite coating; electrodeposition; corrosion resistance; anti-fouling performance; simulated oilfield wastewater

1. INTRODUCTION

Oilfield wastewater contains aggressive ions such as chloride ion, sulfate ion and sulfur ion, which can cause inter-granular corrosion and crevice corrosion of pipeline steel [1-4]. In addition, sulfide ions are also easily combined with some elements in pipeline steel to form various sulfides, which further accelerates the corrosion of pipeline steel. Therefore, how to improve the corrosion resistance of pipeline steel in oilfield wastewater has become an urgent problem to be solved.

The surface coating technology is aim to form a coating on the surface of the substrate based on the principle of deposition to improve the surface performance of the substrate. The commonly used surface coating technologies mainly include electrodeposition, spraying, vapor deposition, electroless plating, laser surface treatment and so on [5-10]. Meanwhile, electrodeposition is a popular surface coating technology due to its mature and stable process. Some coatings with good physical and chemical performance prepared by electrodeposition are introduced in many literatures [11-15].

Ni-W alloy coating and Ni-W composite coating possess optimal corrosion resistance which becomes the focus of people's research [16-20]. Our previous studies have confirmed that the electrodeposited Ni-W/PTFE composite coating on the surface of Q345 pipeline steel can effectively block corrosive media and significantly improve the corrosion resistance of Q345 pipeline steel in simulated oilfield wastewater [21]. In this paper, on the basis of previous research, Ni-W/TiO_2 composite coatings were electrodeposited on the surface of Q345 pipeline steel to extremely improve the corrosion resistance and anti-fouling performance of Q345 pipeline steel in simulated oilfield wastewater.

2. EXPERIMENTAL

2.1 Pretreatment of Q345 pipeline steel

Q345 Pipeline steel used in the experiment was purchased from China Shougang Group and cut into several test pieces as substrates that met the requirements by wire cutting technology. After grinding and polishing, the substrate was soaked in alkaline solution (45 g/L sodium hydroxide and 12 g/L sodium carbonate) at 60℃ for 10 min to remove oil completely. Then the substrate was immersed in 10% hydrochloric acid at room temperature to be activated for 1 min. Finally, the substrate was cleaned with deionized water and placed in a drying oven.

2.2 Preparation of simulated oilfield wastewater

Analytical pure sodium chloride, calcium chloride, sodium bicarbonate, sodium sulfate and sodium sulfide were used to prepare simulated oilfield wastewater. The main composition were shown in Table 1. Pure nitrogen was introduced into the prepared simulated oilfield wastewater to remove oxygen for 6 h to make it reach an anaerobic state. Then an appropriate amount of acetic acid was added to adjust the pH value of the simulated oilfield wastewater to keep it neutral.

Table 1. Main composition of simulated oilfield wastewater

Chemical agent	sodium chloride	calcium chloride	sodium bicarbonate	sodium sulfate	sodium sulfide
Concentration ($g \cdot L^{-1}$)	12.6	4.8	0.15	0.08	0.1

2.3 Electrodeposition of Ni-W/TiO_2 composite coatings

The treated Q345 pipeline steel sample was used as the cathode, and the electrolytic nickel plate was used as the anode. The spacing between the two electrodes was set as 30 mm. Four Ni-W/TiO_2 composite coatings were electrodeposited respectively on the surface of Q345 pipeline steel with constant current density 2 A/dm^2 using KPS3040D DC voltage rectifier, and the electrodeposition time was 60 min. The main composition of the solution is as follows: nickel sulfate 24 g/L, sodium tungstate 45 g/L, boric acid 30 g/L, diammonium hydrogen citrate 100 g/L, sodium dodecyl sulfate 60 mg/L. Fluorinated TiO_2 particles were added into the solution in the form of enhanced phase, with concentrations of 1 g/L, 2 g/L, 4 g/L and 6 g/L, respectively. The solution containing TiO_2 particles was firstly subjected to ultrasonic oscillation for 2 h, and then magnetic agitation for 4 h, so that TiO_2 particles were evenly dispersed.

2.4 Characterization and performance testing of Ni-W/TiO_2 composite coatings

2.4.1 Surface morphology and composition characterization

The surface morphology of Ni-W/TiO_2 composite coating was characterized by high-resolution field emission scanning electron microscope (Supra55, Germany), and the composition of Ni-W/TiO_2 composite coating was analyzed by X-ray photoelectron spectroscopy (X-max80, UK). Based on the mass fraction of Ti element and the relative molecular weight relationship between Ti and TiO_2, the content of TiO_2 particles in the composite coating was calculated.

2.4.2 Measurement of contact angle and calculation of surface free energy

An automatic contact angle tester (JC2000D1) was used to measure the contact angle of water droplets on the surface of Ni-W/TiO_2 composite coating. To reduce the error, three drops of 4 μL were dropped on the surface of each sample, and the measurement results were averaged. In addition, the surface free energy of Q345 pipeline steel and different Ni-W/TiO_2 composite coatings was calculated by Owens two-liquid method.

2.4.3 Corrosion resistance testing

An electrochemical workstation (Parstat 2273, USA) was used to test the electrochemical impedance spectra of Q345 pipeline steel sample and the Q345 pipeline steel samples electrodeposited with different Ni-W/TiO_2 composite coatings in simulated oilfield wastewater. Platinum sheet was used as counter electrode, and saturated calomel electrode was used as reference electrode. The test frequency range was 10^5~10^{-2} Hz, and a sinusoidal signal with amplitude of 5 mV was applied. The test data were imported into ZSimpWin software to obtain the charge transfer resistance and maximum phase angle, which were used to evaluate the corrosion resistance of different Ni-W/TiO_2 composite coating.

In addition, Q345 pipeline steel sample and the Q345 pipeline steel samples electrodeposited with different Ni-W/TiO_2 composite coatings were immersed in simulated oilfield wastewater for 14 days. After that, the samples were cleaned and the corrosion products on the surface were cleaned with a rust remover, and then the corrosion morphology was characterized by scanning electron microscopy.

2.4.4 Anti-fouling performance test

Q345 pipeline steel sample and the Q345 pipeline steel samples electrodeposited with different Ni-W/TiO_2 composite coatings were immersed in simulated oilfield wastewater for fouling deposition experiment for 7 days. The samples were cleaned and dried before and after the experiment. An electronic balance (FA2204N, China) was used for weighing and the fouling deposition rate was calculated according to the following equation.

$$DR_{fouling} = \frac{\Delta G}{S \cdot t} \quad (1)$$

Where, DR_{fouling} represents the fouling deposition rate and unit is g/(m^2·h); ΔG represents the mass difference of samples before and after the fouling deposition experiment and unit is g. S represents the sample surface area and unit is m^2; t represents the fouling deposition experiment time and unit is h.

3. RESULTS AND DISCUSSION

3.1 Composition of different Ni-W/TiO_2 composite coatings

Figure 1 shows the composition of different Ni-W/TiO_2 composite coatings. By comparison, different Ni-W/TiO_2 composite coatings all contain Ni, W, Ti and O elements. Among them, Ti element comes from TiO_2 particles added to the solution, which can confirm that TiO_2 particles and Ni-W coating realize co-deposition to form Ni-W/TiO_2 composite coating. The co-deposition mechanism of TiO_2 and metal alloy has been studied in many literatures [22-24]. When the concentration of TiO_2 particles is 1 g/L, the mass fraction of Ti element in the composite coating is low, indicating that few TiO_2 particles are doped in the composite coating. As the concentration of TiO_2 particles increases, the mass fraction of Ti increases, indicating that more TiO_2 particles are doped in the composite coating. In particular, when the concentration of TiO_2 particles reaches 4 g/L, the content of TiO_2 particles in the composite coating is the highest, reaching 3.90%, as shown in Figure 2. The reason is that the increase in the concentration of TiO_2 particles increases the amount of TiO_2 particles in a uniformly dispersed state in the solution. More particles are driven to the deposition surface and co-deposited with Ni-W coating. However, when the concentration of TiO_2 particles is too high, the mass fraction of Ti element decreases, indicating that the amount of TiO_2 particles doped in the composite coating decreases. The reason is that in the case of excessive TiO_2 particles in the plating solution, the agglomeration effect is easy to be dominant, which leads to the reduction of TiO_2 particles in the composite coating.

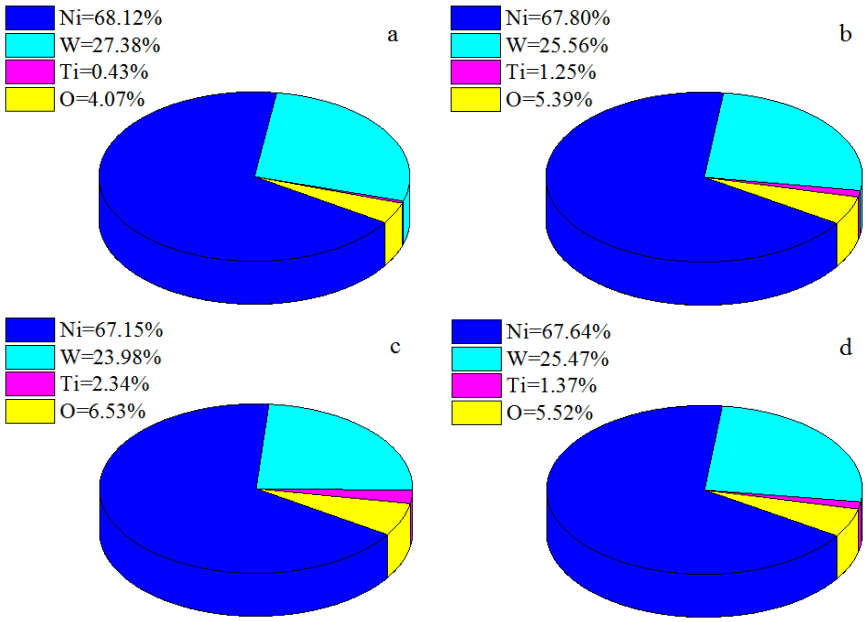

Figure 1. Composition of different Ni-W/TiO_2 composite coatings: a-Ni-W/TiO_2 composite coating (concentration of TiO_2 particles 1 g/L); b-Ni-W/TiO_2 composite coating (concentration of TiO_2 particles 2 g/L); c-Ni-W/TiO_2 composite coating (concentration of TiO_2 particles 4 g/L); d-Ni-W/TiO_2 composite coating (concentration of TiO_2 particles 6 g/L)

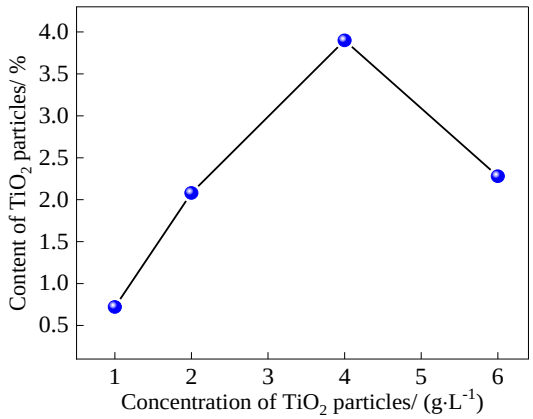

Figure 2. Content of TiO_2 particles in different Ni-W/TiO_2 composite coatings

3.2 Surface morphology of different Ni-W/TiO_2 composite coatings

Figure 3 shows the surface morphology of Q345 pipeline steel and different Ni-W/TiO_2 composite coatings. It can be seen that different Ni-W/TiO_2 composite coatings electrodeposited on the surface of Q345 pipeline steel shows a cellular morphology, and the shape of the unit cell is similar but the size is not uniform. The cellular morphology of Ni-W composite coating has also been reported in some literatures [25-27]. As shown in Figure 3(b), when the concentration of TiO_2 particles is 1 g/L,

the unit cell diameter of the composite coating is larger. The reason is that the promoting effect on crystal nucleation and the inhibiting effect on unit cell growth are not significant when the concentration of TiO_2 particles is low. As the concentration of TiO_2 particles increases to 4 g/L, the unit cell diameter of the composite coating decreases and the density increases gradually. The reason is that the increase in the concentration of TiO_2 particles enables more particles to be co-deposited with Ni-W coating, which reduces the activation energy of crystal nucleation and promotes nucleation. In addition, the TiO_2 particles dispersed in the composite coating can also achieve heterogeneous nucleation, which also has a certain inhibitory effect on the growth of the unit cell, so that the diameter of the unit cell is reduced. However, when the concentration of TiO_2 particles is too high, the unit cell diameter of the composite coating increases and the compactness decreases. This is due to the agglomeration effect of excess TiO_2 particles, which reduces the content of TiO_2 particles in the composite coating and weakens the inhibition of unit cell growth. The agglomeration effect of TiO_2 particles has been reported by some scholars [28-30].

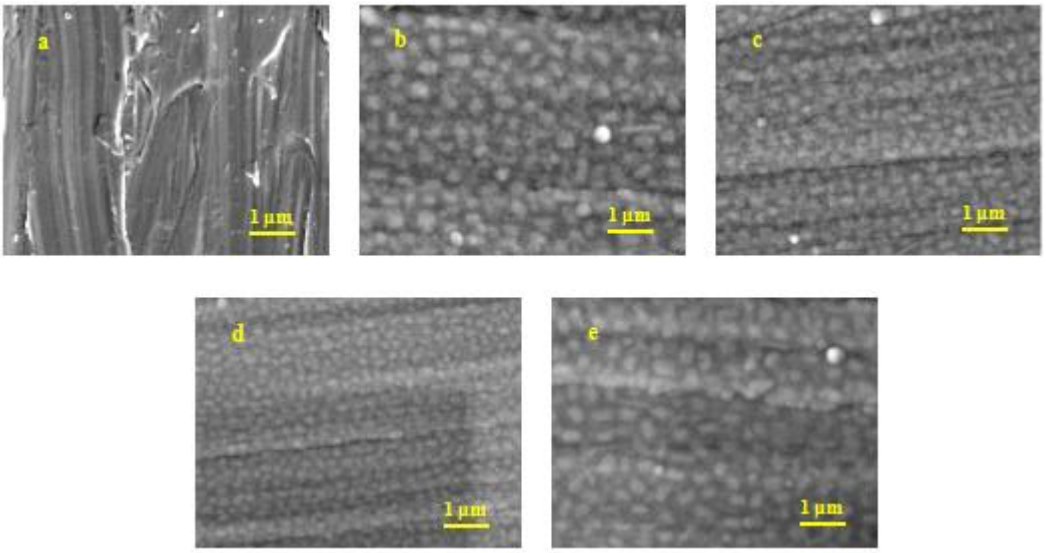

Figure 3. Surface morphology of Q345 pipeline steel and different Ni-W/TiO_2 composite coatings: a-pipeline steel Q345; b-Ni-W/TiO_2 composite coating (concentration of TiO_2 particles 1 g/L); c-Ni-W/TiO_2 composite coating (concentration of TiO_2 particles 2 g/L); d-Ni-W/TiO_2 composite coating (concentration of TiO_2 particles 4 g/L); e-Ni-W/TiO_2 composite coating (concentration of TiO_2 particles 6 g/L)

3.3 Contact angle and surface free energy of different Ni-W/TiO_2 composite coatings

Figure 4 shows the contact angle of water droplet on the surface of Q345 pipeline steel and different Ni-W/TiO_2 composite coatings, while Figure 5 shows the surface free energy of Q345 pipeline steel and different Ni-W/TiO_2 composite coatings. Combined with Figure 4 and Figure 5, it can be seen that the contact angle of Q345 pipeline steel is less than 90°, and the surface free energy is the highest, about 43.25 mN/m. Compared with Q345 pipeline steel, the contact angle and surface free

energy of different Ni-W/TiO_2 composite coatings are different. The free energy shows a trend of first decreasing and then increasing.

The analysis shows that the surface free energy of the fluorinated TiO_2 particles with hydrophobic groups is very low. TiO_2 particles dispersed in the composite coating reduces its surface free energy and weakens its affinity for water droplet, thus inhibiting the spread of water droplet on the surface of the composite coating.

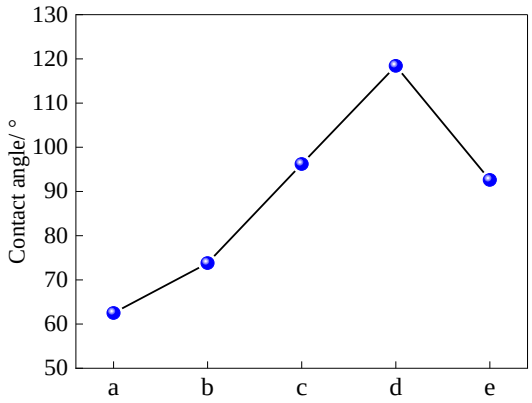

Figure 4. Contact angles of water droplets on Q345 pipeline steel and different Ni-W/TiO_2 composite coatings: a-pipeline steel Q345; b-Ni-W/TiO_2 composite coating (concentration of TiO_2 particles 1 g/L); c-Ni-W/TiO_2 composite coating (concentration of TiO_2 particles 2 g/L); d-Ni-W/TiO_2 composite coating (concentration of TiO_2 particles 4 g/L); e-Ni-W/TiO_2 composite coating (concentration of TiO_2 particles 6 g/L)

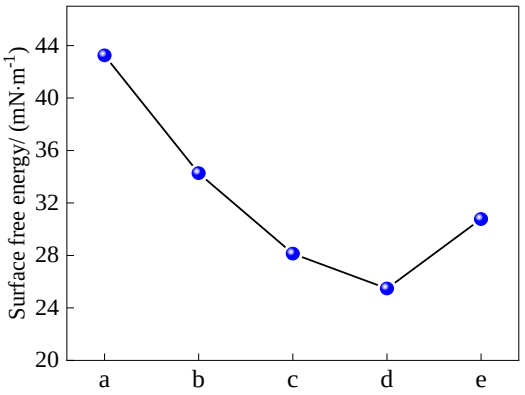

Figure 5. Surface free energy of Q345 pipeline steel and different Ni-W/TiO_2 composite coatings: a-pipeline steel Q345; b-Ni-W/TiO_2 composite coating (concentration of TiO_2 particles 1 g/L); c-Ni-W/TiO_2 composite coating (concentration of TiO_2 particles 2 g/L); d-Ni-W/TiO_2 composite coating (concentration of TiO_2 particles 4 g/L); e-Ni-W/TiO_2 composite coating (concentration of TiO_2 particles 6 g/L)

As the concentration of TiO_2 particles increases, the amount of TiO_2 particles doped in the composite coating increases, which effectively reduces the surface free energy of the composite

coating and reduces the contact area with water droplet, thus the contact angle increases. In particular, the Ni-W/TiO_2 composite coating prepared with the concentration of TiO_2 particles 4 g/L has a minimum surface free energy of 25.48 mN/m, and its contact angle is close to 120°, showing good hydrophobicity. However, when the concentration of TiO_2 particles is too high, the agglomeration effect leads to the reduction of TiO_2 particles doped in the composite coating, so that the effect of reducing the surface free energy of the composite coating is not significant. As a result, the composite coating shows a strong affinity for water droplet, so the contact angle decreases. The relationship between hydrophobicity and surface free energy is stated by some researchers [31-32].

3.4 Corrosion resistance of different Ni-W/TiO_2 composite coatings

Figure 6 shows the electrochemical impedance spectra of Q345 pipeline steel and different Ni-W/TiO_2 composite coatings in simulated oilfield wastewater. It can be seen from Figure 6 that the capacitive arc radius and maximum phase angle of different Ni-W/TiO_2 composite coatings are larger than that of Q345 pipeline steel.

The charge transfer resistance can reflect the difficulty of charge transfer process between the composite coating and the corrosive medium in the simulated oilfield wastewater. The maximum phase angle reflects the blocking effect of the composite coating on the corrosive medium in the simulated oilfield wastewater, which are both used as the evaluation index of corrosion resistance. In general, the larger the arc radius, the higher the charge transfer resistance. The maximum the phase angle, the better the corrosion resistance of composite coating. As can be seen from Table 2, the Ni-W/TiO_2 composite coating prepared with the concentration of TiO_2 particle 4 g/L has the highest charge transfer resistance $6.4\times10^3\ \Omega\cdot cm^2$, which is about 1.8 times higher than Q345 pipeline steel.

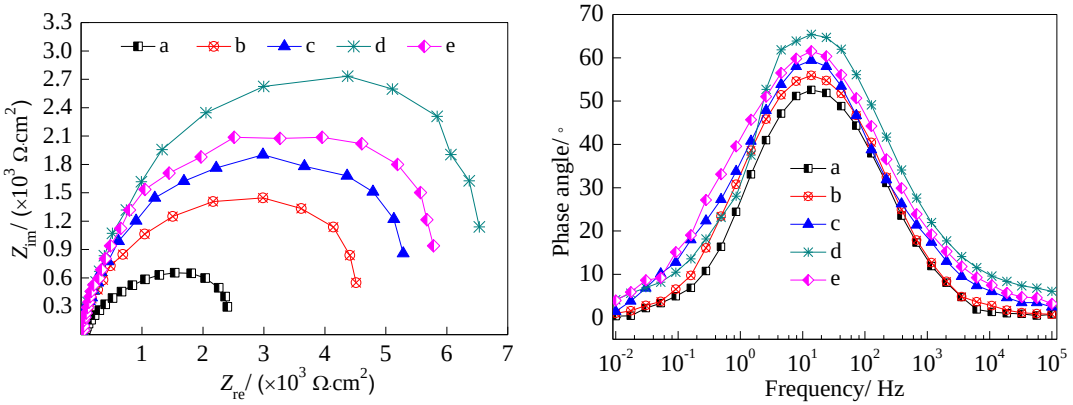

(a) Nyquist spectrum (b) Frequency-phase angle spectrum

Figure 6. Electrochemical impedance spectra of Q345 pipeline steel and different Ni-W/TiO_2 composite coatings in simulated oilfield wastewater: a-pipeline steel Q345; b-Ni-W/TiO_2 composite coating (concentration of TiO_2 particles 1 g/L); c-Ni-W/TiO_2 composite coating (concentration of TiO_2 particles 2 g/L); d-Ni-W/TiO_2 composite coating (concentration of TiO_2 particles 4 g/L); e-Ni-W/TiO_2 composite coating (concentration of TiO_2 particles 6 g/L)

Compared with Q345 pipeline steel, the maximum phase angle reaches 65.3°, which increases by about 24.2%. It can be concluded that the composite coating has the best corrosion resistance and can significantly improve the corrosion resistance of Q345 pipeline steel in simulated oilfield wastewater. The reason is that the composite coating has tight cell bonding and relatively compact surface, which effectively prevents the infiltration of corrosive medium in simulated oilfield wastewater into its interior and presents high electrochemical corrosion resistance. In addition, the composite coating has a lower surface free energy, which can reduce the contact area with the corrosive medium in the simulated oilfield wastewater, resulting in better corrosion resistance. However, when the concentration of TiO_2 particles is low or too high, the surface free energy of the composite coating is large due to the decrease of TiO_2 particles content and the ability to prevent the corrosive medium from penetrating into its interior decreases.

Table 2. Fitting results of electrochemical impedance spectra

Samples	Charge transfer resistance/ ($\Omega \cdot cm^2$)	Maximum phase angle/ °
Q345 pipeline steel	2.3×10^3	52.6
Ni-W/TiO_2 composite coating (concentration of TiO_2 particles 1 g/L)	4.2×10^3	56.0
Ni-W/TiO_2 composite coating (concentration of TiO_2 particles 2 g/L)	5.0×10^3	59.4
Ni-W/TiO_2 composite coating (concentration of TiO_2 particles 4 g/L)	6.4×10^3	65.3
Ni-W/TiO_2 composite coating (concentration of TiO_2 particles 6 g/L)	5.6×10^3	61.5

3.5 Anti-fouling performance of different Ni-W/TiO_2 composite coatings

Figure 7 shows the fouling deposition rate of Q345 pipeline steel and different Ni-W/TiO_2 composite coatings in simulated oilfield wastewater. It can be seen from Figure 7 that the fouling deposition rate on the surface of Q345 pipeline steel is relatively fast, close to 3.6×10^{-2} g/(m^2·h). However, the fouling deposition rate on the surface of different Ni-W/TiO_2 composite coatings is lower than that of Q345 pipeline steel. With the increase of TiO_2 particle content in the composite coating, the fouling deposition rate firstly decreases and then increases. Many studies have shown that the surface free energy of the coating is closely related to the fouling deposition rate, and low surface free energy can effectively inhibit fouling deposition. The Ni-W/TiO_2 composite coating completely covers the Q345 pipeline steel, which reduces the surface free energy and improves the anti-fouling performance of Q345 pipeline steel in simulated oilfield wastewater. In particular, the Ni-W/TiO_2 composite coating prepared with the concentration of TiO_2 particle 4 g/L has the lowest fouling deposition rate, which is about 2.0×10^{-2} g/(m^2·h), resulting in excellent anti-fouling performance.

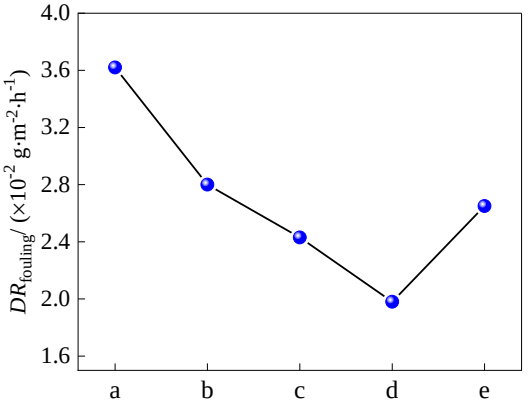

Figure 7. Fouling deposition rate of Q345 pipeline steel and different Ni-W/TiO_2 composite coatings in simulated oilfield wastewater: a-pipeline steel Q345; b-Ni-W/TiO_2 composite coating (concentration of TiO_2 particles 1 g/L); c-Ni-W/TiO_2 composite coating (concentration of TiO_2 particles 2 g/L); d-Ni-W/TiO_2 composite coating (concentration of TiO_2 particles 4 g/L); e-Ni-W/TiO_2 composite coating (concentration of TiO_2 particles 6 g/L)

Figure 8 shows the surface morphology of Q345 pipeline steel and different Ni-W/TiO_2 composite coatings immersed in simulated oilfield wastewater for 7 days. As shown in Figure 8(a), the fouling deposited on the surface of Q345 pipeline steel is concentrated, which further confirms that its anti-fouling performance is poor.

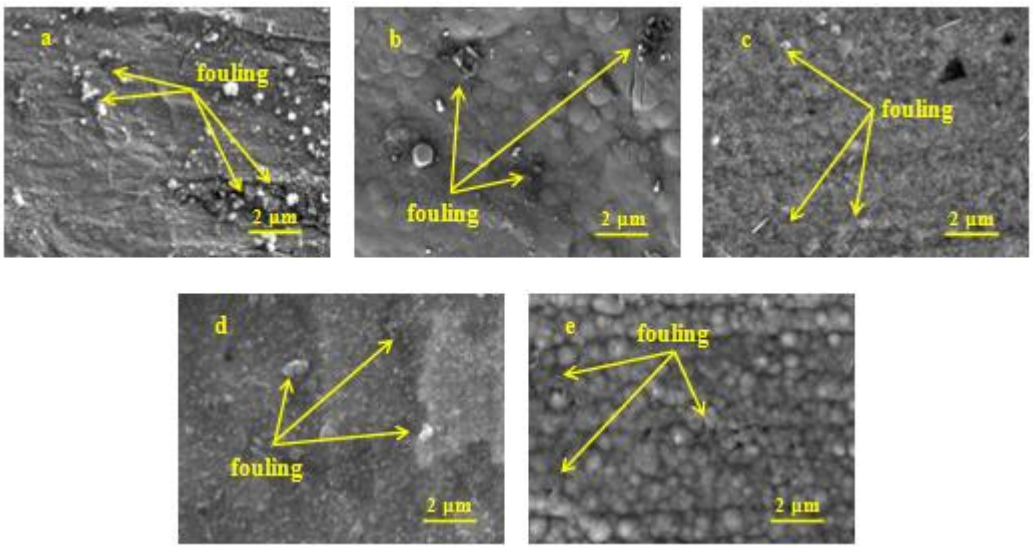

Figure 8. Surface morphology of Q345 pipeline steel and different Ni-W/TiO_2 composite coatings immersed in simulated oilfield wastewater for 7 days: a-pipeline steel Q345; b-Ni-W/TiO_2 composite coating (concentration of TiO_2 particles 1 g/L); c-Ni-W/TiO_2 composite coating (concentration of TiO_2 particles 2 g/L); d-Ni-W/TiO_2 composite coating (concentration of TiO_2 particles 4 g/L); e-Ni-W/TiO_2 composite coating (concentration of TiO_2 particles 6 g/L)

As shown in Figure 8(b) and Figure 8(e), when the concentration of TiO_2 particles is low or too high, some fouling is also deposited on the surface of the composite coating, but it is sparsely distributed. As shown in Figure 8(d), when the concentration of TiO_2 particles is 4 g/L, few fouling deposited on the surface of the composite coating, which further confirms that its anti-fouling performance is the best. The reason is that the composite coating is relatively compact and has the lowest surface free energy, and it is difficult for insoluble metal salts in simulated oilfield wastewater to obtain sufficient energy from the composite coating surface to deposit in the form of crystals. Some articles also reported that the anti-fouling performance of material is mainly related to the free energy and wettability of material surface [33-37]. Reducing the surface free energy and increasing anti-wetting performance can improve the anti-fouling performance of materials which support the conclusions in the paper.

4. CONCLUSIONS

Ni-W/TiO_2 composite coatings were electrodeposited on the surface of Q345 pipeline steel to extremely improve the corrosion resistance and anti-fouling performance of Q345 pipeline steel in simulated oilfield wastewater. The major conclusions are as follows:

(1) Proper concentration of TiO_2 particles can drive more particles to reduce the activation energy of crystallization nucleation and promote nucleation in the composite coating, so that the surface of the composite coating tends to be compact and the surface free energy is reduced, resulting in the improvement of corrosion resistance and anti-fouling performance.

(2) When the TiO_2 particle concentration is 4 g/L, the cellular morphology of Ni-W/TiO_2 composite coating are closely bonded and the surface is relatively compact, and the content of TiO_2 particles reaches 3.90%. The composite coating has the lowest surface free energy of 25.48 mN/m, the highest charge transfer resistance of $6.4\times10^3\ \Omega\cdot cm^2$ and the maximum phase angle approximate 65.3°. Moreover, the Ni-W/TiO_2 composite coating prepared with the concentration of TiO_2 particles 4 g/L shows excellent corrosion resistance and anti-fouling performance, and it can effectively improve the corrosion resistance and anti-fouling performance of Q345 pipeline steel in simulated oilfield wastewater.

References

1. M. Wasim and M. B. Djukic, *J. Nat. Gas Sci. Eng.*, 100 (2022) 104467.
2. K. J. Kere and Q. D. Huang, *Int. J. Press. Vessels Pip.*, 24 (2022) 104656.
3. A. Thoriya, T. Vora and P. Nyanzi, *Mater. Today:. Proc.*, 23 (2021) 112030.
4. J. Kec, I. Cerny, A. Poloch, B. Kysela and M. Poupa, *Procedia Struct. Integrity*, 37 (2022) 598.
5. Y. D. Yu, W. Li, J. W. Lou, H. L. Ge, L. X. Sun, L. Jiang and G. Y. Wei, *Rare Met.*, 31 (2012) 125.
6. S. Ghosh, *Thin Solid Films*, 669 (2019) 641.
7. J. Martin, K. Akoda, V. Ntomprougkidis, O. Ferry, A. Maizeray, A. Bastien, P. Brenot, G. Ezoo and G. Henrion, *Surf. Coat. Technol.*, 392 (2020) 125756.
8. B. W. Lv, X. S. Zhou, C. Wang, X. F. Zhang, Z. L. Qu, B. S. Xu, Y. G. Wang and D. N. Fang,

Ceram. Int., 18 (2022) 1016.
9. B. H. Zhang, J. Chen, P. F. Wang, B. T. Sun and Y. Cao, *J. Mater. Sci. Technol.*, 111 (2022) 111.
10. S. Zhu, *Int. J. Electrochem. Sci.*, 15 (2020) 5352.
11. Y. D. Yu, G. Y. Wei, H. L. Ge, L. Jiang and L. X. Sun, *Surf. Eng.*, 33 (2017) 483.
12. B. W. Yue, G. M. Zhu, Y. W. Wang, J. B. Song, Z. Chang, N. N. Guo and M. G. Xu, *J. Electroanal. Chem.*, 910 (2022) 116146.
13. C. S. Lopes, I. C. Rigoli, C. A. D. Rovere, C. L. F. Rocha and C. A. C. Souza, *J. Mater. Sci. Technol.*, 17 (2022) 852.
14. Y. Deo, R. Ghosh, A. Nag, D. V. Kumar, R. Mondal and A. Banerjee, *Electrochim. Acta*, 399 (2021) 139379.
15. J. G. Liu, X. T. Fang, C. Y. Zhu, X. Xing, G. Cui and Z. L. Li, *Colloids Surf., A*, 607 (2020) 125498.
16. D. Figuet, A. Billard, C. Savall, J. Creus, S. Cohendoz and J. L. Grosseau-Poussard, *Mater. Chem. Phys.*, 276 (2022) 125332.
17. H. J. Li, Y. He, P. Y. Luo, Y. Fan, T. He, Y. H. Zhang, Y. X. Xiang, Y. H. He and R. X. Song, *Surf. Coat. Technol.*, 421 (2021) 127413.
18. B. S. Li, W. W. Zhang, D. D. Li, J. J. Wang, W. Chen and Y. Y. Liu, *Ceram. Int.*, 45 (2019) 13242.
19. Y. Boonyongmaneerat, K. Saengkiteeiyut, S. Saenapitak and S. Sangsuk, *J. Alloys Compd.*, 506 (2010) 151.
20. Y. H. Hu, Y. D. Yu, H. L. Ge, G. Y. Wei and L. Jiang, *Int. J. Electrochem. Sci.*, 14 (2019) 1649.
21. Y. H. Li, *Int. J. Electrochem. Sci.*, 17 (2022) 220340.
22. W. T. Chiu, C. Y. Chen, T. F. M. Chang, T. Hashimoto, H. Kurosu and M. Sone, *Electrochim. Acta*, 294 (2019) 68.
23. M. Uysal, H. Algul, E. Duru, Y. Kahraman, A. Alp and H. Akbulut, *Surf. Coat. Technol.*, 410 (2021) 126942.
24. B. Losiewicz, *Mater. Chem. Phys.*, 128 (2011) 442.
25. P. C. Huang, C. C. Chou and L. S. Hsu, *Surf. Coat. Technol.*, 411 (2021) 126980.
26. L. Y. Zhang, C. T. Peng, J. Shi, Y. X. Jin and R. F. Lu, *J. Alloys Compd.*, 828 (2020) 154460.
27. B. S. Li, W. W. Zhang, D. D. Li and J. J. Wang, *Mater. Chem. Phys.*, 229 (2019) 495.
28. H. Kishimoto, A. Suzuki, T. Shimonosono, M. E. Brito, K. Yamaji, T. Horita, F. Munakata and H. Yokokawa, *J. Power Sources*, 199 (2012) 174.
29. S. Tawkaew and S. Supothina, *Mater. Chem. Phys.*, 108 (2008) 147.
30. H. Boran, D. Boyle, I. Altinok, D. Patsiou and T. B. Henry, *Aquat. Toxicol.*, 174 (2016) 242.
31. A. Cervera-Mata, V. Aranda, A. Ontiveros-Ortega, F. Comino, J. M. Martin-Garcia, M. Vela-Cano and G. Delgado, *CATENA*, 196 (2021) 104826.
32. Z. Y. Shi, Z. Q. Liu, H. Song and X. Z. Zhang, *Appl. Surf. Sci.*, 364 (2016) 597.
33. X. W. Li, J. Y. Yan, T. Yu and B. B. Zhang, *Colloids Surf., A*, 642 (2022) 128701.
34. S. Kalla, K. S. Piash and O. Sanyal, *J. Water Process Eng.*, 46 (2022) 102634.
35. S. Y. Li, F. Zhao, Y. P. Bai, Z. P. Ye, Z. J. Feng, X. Liu, S. D. Gao, X. Y. Pang, M. X. Sun, J. H. Zhang, A. J. Dong, W. W. Wang and P. S. Huang, *Chem. Eng. J.*, 431 (2022) 133945.
36. Y. M. L. Chen, K. J. Lu, C. Z. Liang and T. S. Chung, *Chem. Eng. J.*, 429 (2022) 132455.
37. L. B. Zheng, K. Wang, D. Y. Hou, X. L. Jia and Z. C. Zhao, *Desalination*, 526 (2022) 115512.